

Surfactant-induced structures in the heteroepitaxial growth of Co on Cu(111)

This article has been downloaded from IOPscience. Please scroll down to see the full text article.

2001 J. Phys.: Condens. Matter 13 9897

(<http://iopscience.iop.org/0953-8984/13/44/306>)

View [the table of contents for this issue](#), or go to the [journal homepage](#) for more

Download details:

IP Address: 171.66.16.226

The article was downloaded on 16/05/2010 at 15:05

Please note that [terms and conditions apply](#).

Surfactant-induced structures in the heteroepitaxial growth of Co on Cu(111)

S Müller¹, J E Prieto^{2,3}, T Krämer^{1,4}, C Rath¹, L Hammer¹, R Miranda²
and K Heinz¹

¹ Universität Erlangen-Nürnberg, Lehrstuhl für Festkörperphysik, Staudtstr. 7,
D-91058 Erlangen, Germany

² Dpto. Física de la Materia Condensada and Instituto Universitario de Ciencia de Materiales
'Nicolás Cabrera', Universidad Autónoma de Madrid, Cantoblanco, E-28049 Madrid, Spain

E-mail: kheinz@fkp.physik.uni-erlangen.de

Received 20 July 2001, in final form 21 September 2001

Published 19 October 2001

Online at stacks.iop.org/JPhysCM/13/9897

Abstract

The growth of Co on Cu(111) with Pb as a surfactant is found to be accompanied by a considerable surface reconstruction of (4×4) symmetry induced by the surfactant. Its crystallography was investigated by quantitative low-energy electron diffraction (LEED) for an initial and later stage of growth with deposition of 1.3 monolayer (ML) and 7 ML Co, respectively. In the low coverage case the surface reconstruction is rather similar to that of Pb/Cu investigated earlier. It extends deep into the substrate with simultaneous minimization of the Pb layer buckling. The structure seems to be controlled by dominating fcc-stacking characteristic of this early stage of growth. With further cobalt deposition the type of reconstruction changes. For the 7 ML Co film it is restricted to the Pb and top Co layer only with the buckling of the surfactant layer considerably increased. We discuss that this may be attributed to the slightly different lattice parameters of Cu and Co, though the influences of the different stacking involved cannot be ruled out. The top film layer is always reconstructed during the whole growth which might be responsible for the easy exchange processes which take place during the growth and are essential for the layer-by-layer growth as found earlier.

1. Introduction

In the epitaxial growth of ultrathin metallic films on the surfaces of single crystals surface-active agents, i.e. so-called *surfactants*, can play an important role. Though their influence on the growth has been known for a long time in principle [1], the microscopic processes behind them have been largely hidden. Only recently some light was shed on the atomic processes

³ Present Address: Institut für Experimentalphysik, FU Berlin, Arnimallee 14, D-14195 Berlin.

⁴ Present Address: DESY, Notkestr. 85, 22603 Hamburg.

controlling the surfactant action of Pb on the (homoepitaxial) growth of Cu on Cu(111) [2]. It was found that arriving copper atoms are quickly incorporated into the Pb layer where they undergo exchange processes with atoms of the top Cu layer. These processes control the lateral intralayer diffusion of the copper atoms making it much slower than the hopping diffusion which dominates on clean Cu(111) [3]. In contrast, the effect of the surfactant on interlayer diffusion, i.e. on the overcoming of the Ehrlich–Schwoebel barrier at a step edge, appears to be negligible [2]. This is because already in the absence of the surfactant, exchange processes, rather than jumps over the barrier, dominate as described earlier [4]. As a consequence, lead as a surfactant in the case of Cu/Cu(111) makes the ratio of intra- to interlayer diffusion decrease. Eventually, this leads to layer-by-layer growth compared to multilayer growth on the clean surface as observed experimentally [2]. Consistently, homoepitaxial growth on Cu(100) is layer-by-layer even in the absence of surfactants as intralayer diffusion is comparably slow according to a rather large activation barrier (0.4 eV for Cu(100) [5] compared to about 0.03 eV for Cu(111) [6]).

Though this progress of our understanding of the surface-active mechanisms (which may apply not only to Pb/Cu) is substantial, we are still left with many unknowns. In particular, little (if not nothing) is known about the role played by the crystallographic structure of the surfactant–surface combination. This is in spite of the fact that—in the light of the above-described scenario—the competition between exchange and hopping diffusion depends heavily on the surface structure as explicitly shown by calculations of the self-diffusion for the (100), (110) and (111) surfaces of Cu [3]. This structural sensitivity is important in view of the surfactant’s potential to induce a more or less strong modification, i.e. a reconstruction of the surface and so to modify the surface energetics which in turn influences the growth. In fact, a monolayer (ML) of Pb on Cu(111) (equivalent to $\frac{9}{16}$ of the atomic density of a copper layer) induces a substantial substrate reconstruction of (4×4) symmetry. There are large atomic corrugations in the Pb layer as shown experimentally by scanning tunnelling microscopy (STM) [7] and helium-atom scattering [8] and confirmed by calculations using the effective-medium theory (EMT) [7]. Even more, according to EMT the corrugation penetrates the substrate with considerable amplitude extending down to the third copper layer which in fact was found experimentally by quantitative low-energy electron diffraction (LEED) [9].

It has been speculated that the reconstruction might be crucial for the surfactant’s activity [2, 9]. In fact, the mentioned (4×4) superstructure is also characteristic of the heteroepitaxial growth of Co on Pb/Cu(111). Certainly, it is observed in the absence of any substrate reconstruction due to the coincidence mesh given by the ratio of the atomic sizes and to the fact that during growth the lead atoms always float to the surface [10–12]. Yet, it would be surprising if no substrate reconstruction were induced. This is both in view of the experience with Pb/Cu and the fact that the Pb layer would need to undergo a very large buckling.

The (4×4) superstructure prevails during the whole growth, i.e. from low coverages up to many cobalt layers when a full Pb monolayer covers the surface [10]. In the latter case there is nearly ideal layer-by-layer growth from the second ML on, while multilayer growth dominates on the clean substrate [13–15] similar to the homoepitaxial system. The surfactant has almost no influence on the stacking of cobalt layers which switch from fcc stacking in the very early stages of growth to hcp stacking after a few monolayers [10, 14].

In spite of the possible relevance of surfactant-induced reconstruction on the growth of Co on Cu(111), none of the papers published focuses on the crystallographic structures involved during growth. This is certainly due to the relatively large (4×4) unit cell which allows for rather complex types of reconstructions as has been found for (4×4) -Pb/Cu(111) [9]. We have extended our investigations of the latter system to the quantitative analysis of (4×4) -Pb/Co/Cu(111) and present the results in this paper. By applying quantitative LEED

with input about the surface morphology from STM investigations published earlier [10] we retrieve the crystallographic structure involved in the growth. We hereby concentrate on two stages, namely an early stage of growth with a total cobalt coverage equivalent to 1.3 ML (corresponding to coexisting domains with single and double cobalt layers) and a comparably advanced stage with 7 ML Co. Comparison is made to the structure of (4×4) -Pb/Cu(111) [9]. It turns out that the structure of Pb/7 ML Co/Cu(111) is significantly different from that of Pb/Cu(111), while that of Pb/1.3 ML Co/Cu(111) exhibits strong similarities.

2. Experimental details

An ultrahigh vacuum chamber equipped with facilities for STM and LEED was used for the experiments as described in more detail earlier [10]. The electrochemically polished Cu(111) crystal was cleaned *in situ* by cycles of ion sputtering and annealing resulting in contaminant-free Auger spectra and a sharp (1×1) LEED pattern with low background. STM images exhibited clean Cu(111) terraces several tens of nanometers wide and separated by monoatomic steps. Deposition of about a monolayer of Pb was made by resistive heating of the material held in a Ta basket. This was followed by Co deposition accomplished by heating a high-purity cobalt rod through electron bombardment. In both cases the sample was held at room temperature during deposition. The adsorbate Pb/Cu was annealed at 420 K in order to make the lead form a single monolayer [9]. Annealing of the cobalt adsorbate was avoided in order to suppress intermixing of Cu and Co. For the coverage calibration of Pb and Co the Auger signals of the materials involved were used. For more details we refer to earlier work [9, 10, 14].

Starting with the Pb/Cu(111) system, a (4×4) LEED pattern appears which prevails during the whole growth of Co films, however, with spot intensities varying with coverage. As for the clean and Pb-covered substrate, the LEED pattern of the 1.3 ML Co coverage exhibits threefold symmetry at normal incidence of the primary beam. It transforms to sixfold symmetry at 7 ML coverage as shown in detail in [10]. The use of the LEED optics as a retarding field spectrometer for Auger electron spectroscopy (AES) shows that the Pb signal remains constant in amplitude while that of Cu decreases with increasing Co deposition [10]. This is indicative of a continuous and complete flow of Pb to the surface, i.e. the surface is always covered by the Pb monolayer with the growing Co film below.

LEED intensity versus energy spectra, $I(E)$, were recorded for the mentioned selected stages of growth, i.e. for Co coverages of 1.3 and 7 ML, with the sample at room temperature in each case. Applying an automated, computer-controlled video technique [16] the data were taken at normal incidence of the primary beam in steps of 0.5 eV in the energy range 50–360 eV for the 1.3 ML sample and 50–400 eV for the 7 ML sample. Only spots with intensities sufficiently high to be measured reliably were made to enter the database. In order to improve the signal-to-noise ratio of the data and to reduce the influence of some residual sample misalignment and inhomogeneities of the luminescent screen, spectra of symmetrically equivalent beams were averaged. For the 1.3 ML sample this resulted in symmetry-inequivalent spectra of three integer and four fractional order spots amounting to total energy ranges of 425 and 790 eV, respectively, giving a grand total of $\Delta E = 1215$ eV. The spectra for the 7 ML sample stem from three integer and three fractional order spots with energy ranges of 520 and 450 eV, respectively, yielding a grand total of $\Delta E = 970$ eV. The reduced number of beams in the latter case is due to the higher, i.e. sixfold rotational symmetry of the diffraction pattern. This can be either due to the growth of cobalt in fcc-twins or, more likely, to predominant hcp stacking of the cobalt layers. In the latter case the presence of single height atomic steps (as observed by STM [10]) is equivalent to domains rotated by 60° with

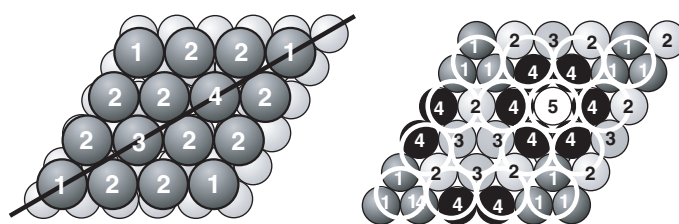


Figure 1. Top view of the Pb-induced (4×4) unit cell. Large balls represent Pb atoms in the top layer, smaller atoms stand for Co or Cu atoms in the layers below. The black line marks the assumed mirror plane. The atomic labels are used below to identify the various atoms.

respect to each other, so that the incoherent adding of their intensities produces the sixfold symmetric diffraction pattern observed.

3. Intensity analyses—computations and structural search

Similar to the case of (4×4)-Pb/Cu(111) [9] the full dynamical intensity analyses of the (4×4) phases of Pb/1.3 ML Co/Cu(111) and of Pb/7 ML Co/Cu(111) are rather demanding. This is due to the large number of atoms in the (4×4) unit cell as illustrated in figure 1. There are 9 Pb atoms and 16 Co or Cu atoms per atomic layer in the surface unit cell. Though the superstructure has rather incommensurate features due to the Pb lattice being mismatched to that of the substrate (many different coordinations between lead and substrate atoms) it happens to be commensurate to the Pb coverage chosen. Therefore, the substrate's mirror plane most likely also holds for the overlayer, so that there are only four inequivalent Pb atoms (as indicated in figure 1) and five non-equivalent atoms in Co or Cu layers below [9]. Furthermore, substantial lateral reconstructive movements of atoms are unlikely compared to vertical movements due to the close atomic packing within the layers when undistorted, i.e. the reconstruction should be dominated by the vertical buckling of layers. In the following the choice of the surface unit cell is always made as displayed in figure 1 (corresponding to that used in our previous paper on Pb/Cu [9]), i.e. there will always be the same coordination of the Pb layer to the hexagonal layer below independent of the way deeper layers are stacked. This allows us to use the same numbering of atoms. It is then only by the stacking of the second substrate layer that one of the hollow-site Pb atoms (no 1 or 3) will happen to be in a fcc or hcp site.

With the vertical buckling of layers dominating the reconstruction, one can start from unbuckled (unreconstructed) layers and then displace the various atoms vertically by which procedure rigid layer displacements, i.e. relaxations of (average) vertical spacings $d_{i,i+1}$ between the i th and $(i + 1)$ th neighbored layers are also covered. For the calculation of the corresponding intensity spectra the perturbation method tensor LEED (TLEED) [17–19] was applied using a special program package [20]. As the method always refers to a certain reference structure and is valid only within a certain parameter-space environment of this reference, special care was taken that a new reference was calculated as soon as this environment was left. With TLEED allowing for any (small) atomic displacements, atomic thermal vibrations also could easily be taken into account in parallel. They were assumed to be isotropic. Possible intermixing of Pb and Co or Cu was checked by substituting their atomic scattering matrices within the framework of TLEED [21, 22]. For the structural search a frustrated simulated annealing procedure was used [23].

For the intensity calculations a total of 11 spin-averaged phase shifts was used to describe the scattering of the different atoms. They were corrected to consider isotropic atomic vibrations using the bulk Debye temperatures for Co and Cu, i.e. 450 and 343 K, respectively. For the surfactant layer on top, a Debye temperature of 110 K was applied, which resulted as the best-fit value for the system Pb/Cu(111) [9]. The electron attenuation was described by a constant imaginary part of the inner potential, $V_{0i} = 5$ eV. Its real part V_{0r} (also taken as energy independent) was varied in the course of the theory–experiment fit. For a quantitative measure of the latter the Pendry R -factor [24] was applied. It was also used to guide the structural search. Its variance, $\text{var}(R_P) = R_P \sqrt{8V_{0i}/\Delta E}$ (with R_P the best-fit, i.e. minimum Pendry R -factor), was used to estimate the error limits of the parameters varied in the structural search [24].

4. Results

For both the stages of growth investigated we can take advantage of the fact that in spite of the strong surface reconstruction to be expected, the most influential structural parameter determining the intensities of integer order beams is the stacking of layers [25]. The structure of the intensity spectra of these beams is not drastically modified by the reconstruction as has also been observed in the study of (4×4) -Pb/Cu(111) [9]. As illustrated in figure 2 this also holds for Pb/Co(0001), whose spectra together with those of Co were recorded in other work [10]. The integer beam spectra for Cu and Pb/Cu as well as for Co and Pb/Co (which was investigated independently) are very similar and the three and sixfold symmetry, respectively, is saved. The observation that integer order beam spectra are not drastically affected *either* by the substrate reconstruction *or* by the presence of an overlayer of strongly scattering atoms (Pb) is due to the rather large unit cell. This will be discussed in more detail at the end of section 4.1.

Not surprisingly, the Pb/7 ML Co/Cu data are also close to those of Pb/Co indicating predominant hcp stacking already at this point (the origin of the small discrepancies will be addressed at the end of section 4.1). The cobalt film can also be expected to assume its native hcp stacking for large film thickness as shown for epitaxial Co films on clean Cu(111) [14]. Though the observed sixfold symmetry could also be due to the formation of fcc twins (as detected for the growth of Co on Cu(111) when capped with two copper layers [14]) this possibility can be ruled out as the spectra would be rather different [14]. For the 1.3 ML film, however, we cannot foresee the stacking either from the physics or by the inspection of the above spectra. On the one hand, the strictly fcc-stacked copper substrate must be expected to influence the stacking in the film which starts to grow. On the other hand, the LEED electrons probe the film, the interface and the substrate and so contributions from possibly differently stacked layers mix.

In the following we first address the structure of the 7 ML Co film, in particular as this turns out to be the structurally simpler case. Subsequently, we will focus on the phase with 1.3 ML cobalt deposited.

4.1. Structure of (4×4) -Pb/7 ML Co/Cu(111)

As a consequence of the dominant influence of the layer stacking on the intensities of integer order beams, these spectra can be easily analysed. The result is that the Co layers are strictly hcp stacked rather than fcc-twin grown. This is consistent with the similarity of the spectra with those measured for Pb/Co(0001) [10] as demonstrated in figure 2. We have to note,

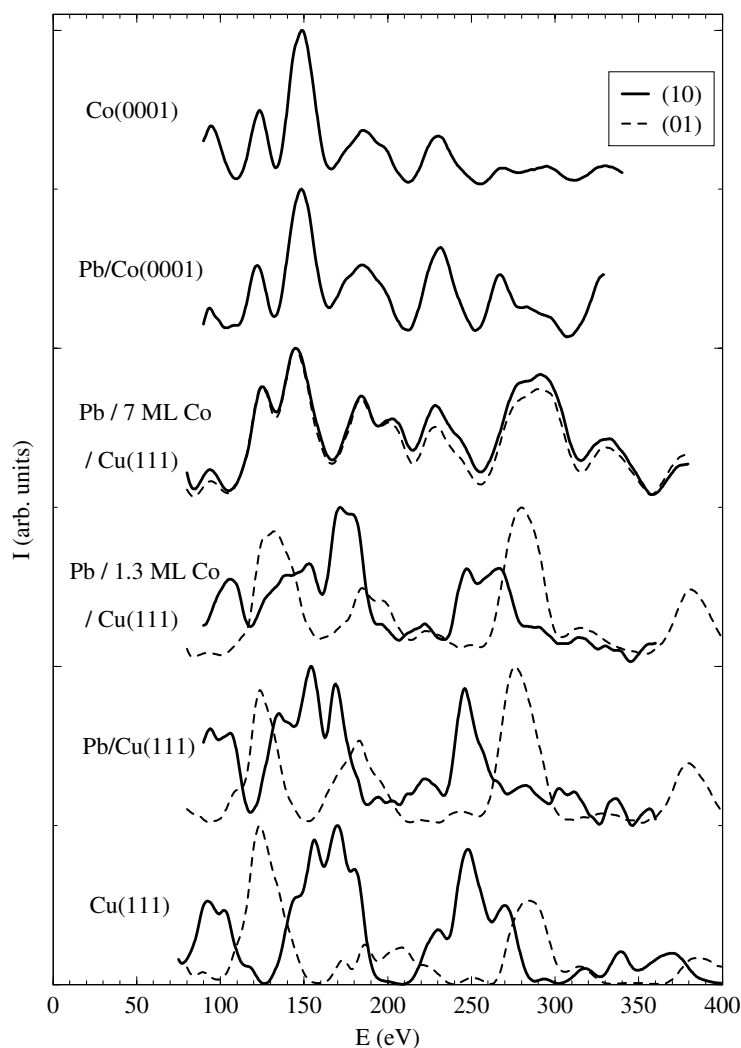


Figure 2. Survey of (10) and (01) beam spectra normalized to the same height for different phases demonstrating that the intensities of integer order spots are dominated by layer stacking and little affected by surface reconstruction.

however, that hcp stacking may not hold for the very interface region as the influence of the latter is hidden by electron attenuation.

The variation of vertical atomic coordinates to find the character and extent of the reconstruction was made stepwise, i.e. restricted to the Pb layer in the first step and including more layers in subsequent steps. Of course, in each step the parameters of the layers already varied in the preceding step had to be varied again. It turned out that a good fit between calculated and experimental data of integer order beams resulted only by adding contributions of about 20% of the surface uncovered by Pb. This is similar to the situation encountered for Pb/Cu [9] and is not surprising in view of the fact that the same amounts of Pb were deposited in both cases. Obviously the deposition of an uncomplete Pb layer was by an experimental accident; the solution of Pb into the substrate can be ruled out as tested by

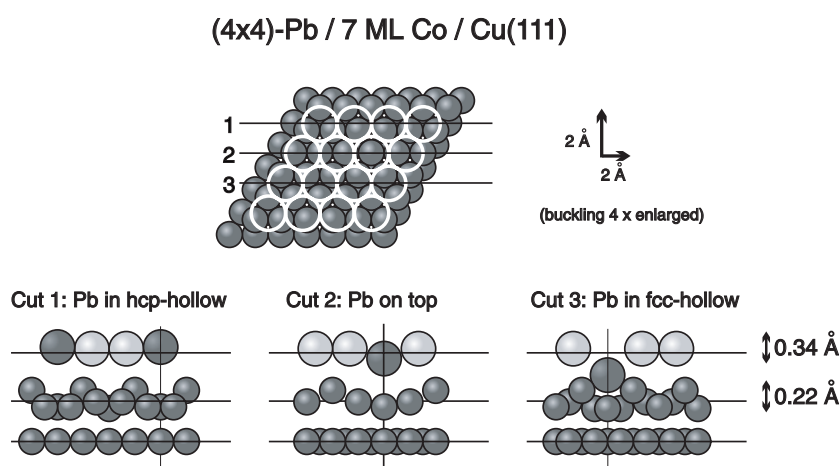


Figure 3. Top and side views of the structure of (4×4) -Pb/7 ML Co/Cu(111). The side views correspond to vertical cuts as indicated in the top view. Pb atoms (large balls) residing in high symmetry sites (on top, fcc- or hcp-hollow) are indicated by darker shading. Note that the vertical scale is enlarged and the buckling of layers four times amplified in order to be clearly seen.

TLEED. Besides the R -factor fit, the ratio between the energy-averaged intensity spectra of fractional and integer order spots also fits only to the experiment when a mixture with a 20% surface patch uncovered by lead is considered (more details on that point will be discussed at the end of this section). With that considered, the structural search procedure quickly converged producing a minimum $R_P = 0.19$ which is a favourable value in view of the complexity of the structure involved. The experimental ratio between the energy-averaged intensities of fractional and integer order beams ($r_{\text{exp}} = 0.30$) was reproduced in the fit also in good approximation ($r_{\text{calc}} = 0.32$). Similar to the case Pb/Cu, test calculations show that there are no lead atoms intermixed with film atoms.

The analysis shows that the reconstruction does not considerably penetrate the surface. Below the Pb layer (overall buckling amplitude 0.34 Å) only the top cobalt layer is significantly buckled (0.22 Å). Additional variation of atomic positions in the second cobalt layer results in only a very small buckling (0.04 Å). As this too is well within the limits of error, it can be neglected. The scenario of the reconstruction is illustrated by the side views in figure 3 which correspond to the vertical cuts as indicated in the top view (note that the vertical scale is twice as large as the lateral scale and that, additionally, the buckling displacements are enlarged four times to be seen). For the unit mesh chosen, its corner Pb atom (Pb atom no 1 in figure 1) resides in a hcp-hollow site so that the other hollow site (Pb atom no 3) is of fcc type.

For comparison we recall the result retrieved for (4×4) -Pb/Cu(111) obtained earlier [9] and illustrated in the same way as above in figure 4. The reader should note that here the types of hollow sites of Pb atoms are interchanged, i.e. the corner of the Pb atom resides in a fcc-hollow site. Apparently, for Pb/Cu the surfactant-induced reconstruction extends considerably deeper into the surface than for Pb/7 ML Co/Cu and the buckling of the Pb layer is less pronounced.

The displacements of the Pb and Co atoms with respect to the average layer planes are given in table 1 where again the comparison to Pb/Cu is offered (numbers in *italic*). For Pb/7 ML Co/Cu the error estimation for atomic positions using the variance of the R -factor ($\text{var}(R_P) = 0.039$) yields error limits of about ± 0.04 Å for the Pb layer and ± 0.06 Å for

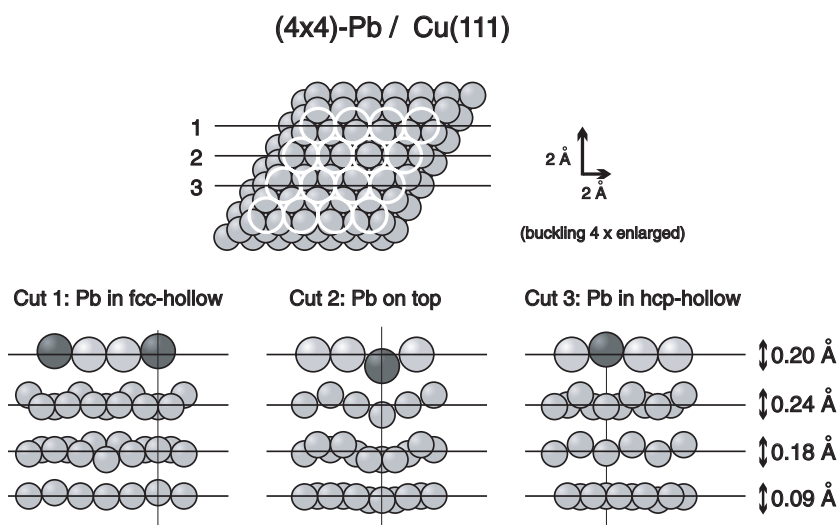


Figure 4. Same as figure 3 but for (4×4) -Pb/Cu(111) according to [9].

Table 1. Vertical displacements of atoms and overall buckling amplitudes in the top few layers of (4×4) -Pb/7 ML Co/Cu(111) compared to (4×4) -Pb/Cu(111) (in italics, as taken from [9]). The numbering of atoms is according to figure 1. Positive (negative) coordinates denote outward (inward) displacements relative to the average plane of the layer.

	Displacements (Å) for atom number					Overall buckling (Å)
	1	2	3	4	5	
Pb layer on						
7 ML Co/Cu(111)	+0.07	+0.05	-0.27	-0.07	-	0.34
<i>Cu(111)</i>	<i>+0.04</i>	<i>0.00</i>	<i>+0.06</i>	<i>-0.14</i>	-	<i>0.20</i>
1st Co layer	-0.08	+0.14	-0.06	-0.00	-0.06	0.22
<i>1st Cu layer</i>	<i>-0.02</i>	<i>+0.12</i>	<i>-0.02</i>	<i>0.00</i>	<i>-0.12</i>	<i>0.24</i>
2nd Co layer	-	-	-	-	-	-
<i>2nd Cu layer</i>	<i>-0.10</i>	<i>-0.03</i>	<i>+0.02</i>	<i>+0.08</i>	<i>-0.02</i>	<i>0.18</i>
3rd Co layer	-	-	-	-	-	-
<i>3rd Cu layer</i>	<i>0.00</i>	<i>-0.01</i>	<i>-0.05</i>	<i>0.00</i>	<i>+0.04</i>	<i>0.09</i>

the first Co layer, so that the coordinates for single atoms are rather uncertain (as already mentioned, we neglect atomic shifts in the second cobalt layer, in particular as errors increase with depth). We emphasize, however, that in spite of the large single-coordinate errors the overall buckling amplitudes of the layers are on much safer grounds as they are necessary to reproduce the experimentally observed intensity level of superstructure spots. The vertical spacings between the average planes of layers for Pb/7 ML Co/Cu amount to $d_{12} = 2.34$ Å, $d_{23} = 1.96$ Å and $d_{34} = 2.05$ Å.

At this point the reliability of the analysis should be addressed. With the reconstruction dominated by the Pb layer (four symmetrically inequivalent atoms) and the top Co layer (five different atoms), there are nine (vertical) coordinates to be determined. As each energy

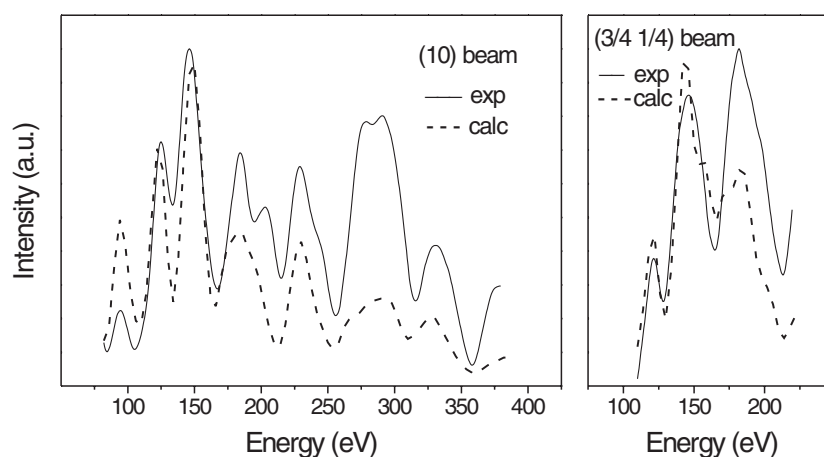


Figure 5. Comparison of experimental and calculated best-fit spectra for a selected integer and fractional order beam of (4×4) -Pb/7 ML Co/Cu(111).

window of width $\delta E = 4V_{oi} = 20$ eV is supposed to carry independent structural information [24] we need at least a database width of $9 \delta E = 180$ eV. So, with $\Delta E = 970$ eV we get a redundancy factor larger than 5, i.e. our structure determination is on safe grounds. The theory–experiment fit is rather favourable not only as judged from the minimum R -factor, $R_p = 0.19$, but also by the visual comparison of calculated and measured spectra which is offered in figure 5 for two selected beams.

As pointed out above, there are some discrepancies between the spectra of a lead film on the surface of a Co(0001) bulk crystal and on the 7 ML Co film on Cu (see figure 2). This is due to the fact that the Pb coverage on the bulk crystal amounts to a full monolayer while that on the film is only 80% of it. This is not only deduced from the R -factor fit, i.e. from the structure of the spectra, but is also consistent with the ratio r of the average intensity levels of fractional and integer spot intensities. As in reconstructed, i.e. Pb-covered domains, the incoming beam is diffracted into a large set of beams according to the (4×4) superstructure, the integer order beams are much less intense than for the lead-free Co surface. As a consequence, r is considerably larger for a fully Pb covered surface ($r \approx 2$ for Pb/Co(0001)) than for a surface only partly covered ($r \approx 0.3$ for Pb/7 ML Co/Cu(111)) as observed. On the other hand, the structure of the $I(E)$ spectra of integer order spots only modestly changes with Pb deposition. This is due to the adlayer's (and the reconstructed surface layers') rather large unit cell which exhibits to some degree even some incommensurate features with the underlying bulk. In any case, the intensities of only the fourth order spot of the surface add to the intensities of the first integer order spot of the underlying bulk. This explains both, that the mentioned differences in the spectra of figure 2 exist and that they are rather small with respect to the spectral structure of the data in spite of the strongly scattering adlayer and the strong reconstruction it induces (yet, the reader should note that the average intensity level is considerably reduced by the Pb adlayer and that the spectra in figure 2 are normalized to the same height). All the features described are reproduced in the above analysis. Also, we have analysed Pb/Co(0001) and retrieved qualitatively the same structure as for the 7 ML film. Yet, because only a small database is available, the error limits for the structural parameters turn out to be rather large. We therefore do not list these values.

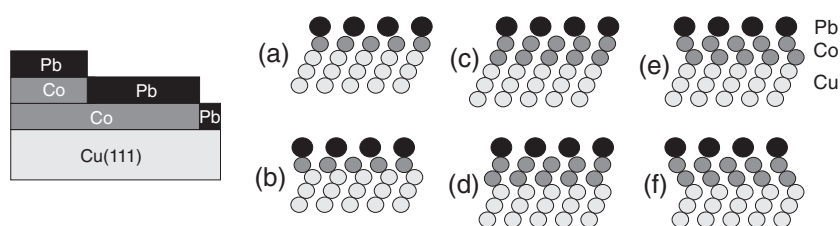


Figure 6. Average surface morphology (left) as resulting from STM [10] and possible layer stackings (a–f) of the one- and two-monolayer domain of (4×4) -Pb/1.3 ML Co/Cu(111). The stacking sequence is displayed along the mirror plane cut indicated in figure 1. Linear stacked arrangements correspond to fcc, zig-zags to hcp stacking. Breaks in the linearity stand for stacking faults.

4.2. Structure of (4×4) -Pb/1.3 ML Co/Cu(111)

Inspection of the STM images for low cobalt coverages [10] suggests that within the terraces separated by substrate steps there are only two to three atomic levels developing with cobalt deposition at room temperature. For the particular case of 1.3 ML Co/Cu(111) the average morphology is according to figure 6 (left part) with three atomic levels exposed. The whole surface lies under a Pb carpet as judged by the always present 4×4 reconstruction, i.e. there are no patches uncovered by lead. This is consistent with the ratio between (energy averaged) intensities of fractional and integer order beams being near unity, both for the experimental value and the eventual best-fit calculation. The weight of the lowest exposed domain is only about 10% of the total surface area. The middle and top level areas are considerably larger with the former exceeding the latter. As the total Co coverage is about 1.3 ML, Co layers can only exist in the top and middle level areas with double and single Co layers, respectively. Yet, even with that information at hand we impossibly hope for an exact LEED structure determination. This is because we need to fit contributions of three domains, each of which is characterized by a possibly different and complex (4×4) reconstruction. Certainly, this is not possible with a database width amounting to not more than $\Delta E = 1215$ eV.

The different stacking possibilities for the two domains containing cobalt layers are displayed in panels (a–f) of figure 6. Fortunately, we know from earlier analyses [14, 26] of the growth of Co on Cu(111) in the absence of the surfactant that the first cobalt layer always proceeds with the fcc stacking dictated by the copper substrate. Only with further cobalt deposited can the stacking change by the introduction of stacking faults, a behaviour not modified by the presence of the surfactant [10]. This allows immediate ruling out of cases (b), (d) and (f) which, of course, make the analysis much easier. Additionally, because of the very similar scattering characteristics and scattering strengths of cobalt and copper and their small lattice misfit we cannot dare to be able to differentiate between cases (a) and (c) at an expected *R*-factor level of the order of 0.2. The two cases (a) and (c) have in common the fact that all layers below lead are fcc stacked. The same holds for the possible domains in which a layer of copper is segregated to the surface (as has been described in [14]), so that, together with the copper bulk, it sandwiches a single cobalt layer. The fcc-stacking below the lead layer also applies to the above-mentioned small domain of 10% of the surface uncovered by cobalt. In view of the fact that the type of stacking largely dominates the intensity spectra [25], we treat all these fcc-stacked areas as a single fcc-domain in the following, while the remaining case (e) in figure 6 is considered as the ‘hcp-domain’. The latter expression is, however, only partly adequate as the domain is better characterized by the presence of a single stacking fault rather than strict hcp-stacking in the substrate. The two differently stacked domains

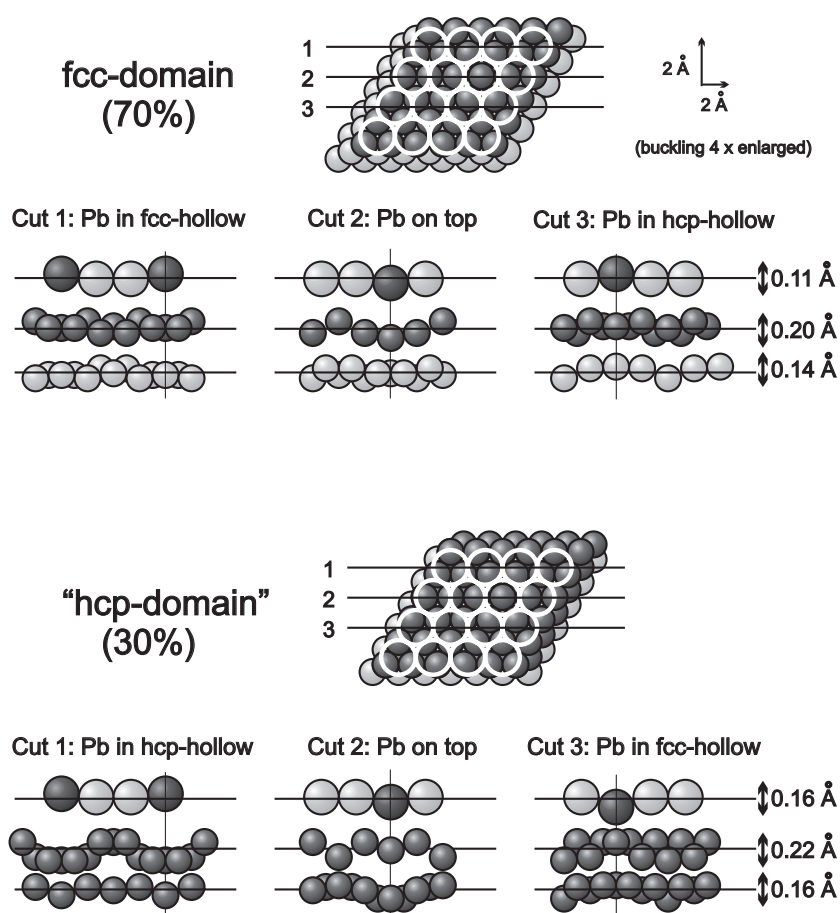
(4x4)-Pb / 1.3 ML Co / Cu(111)

Figure 7. Top and side views of the structures of the fcc-domain (top) and ‘hcp-domain’ (bottom) of (4×4) -Pb/1.3 ML Co/Cu(111). The outlay of the figure is the same as for figure 3.

were made to enter the intensity analysis with adjustable weight, i.e. x for the fcc-domain and $(1 - x)$ for the ‘hcp-domain’. Again, the reconstruction of different layers was allowed step by step. However, in view of the restricted database and the large parameter space (two domains) we did not allow reconstructions in the third substrate layer.

The best fit achieved by the structural search resulted for $x = 0.70$. In both domains the surfactant-induced reconstruction extends to the second substrate layer. There might be some small buckling also in the third layer of each domain which, however, was not considered in the analysis as mentioned above. Again, test calculations showed that there are no Pb atoms left within the film. The structures of the two fcc- and hcp-stacked domains are displayed in figure 7. For simplicity, the fcc-domain is displayed in the figure with a single cobalt layer only, though there can also be contributions of other fcc-stacked combinations as two cobalt layers: a copper followed by a cobalt layer or only copper layers below. The atomic coordinates are summarized in table 2, but we strongly emphasize that the error limits involved

Table 2. Vertical displacements of atoms and overall buckling amplitudes in the top few layers in the two domains of (4×4) -Pb/1.3 ML Co/Cu(111). The numbering of atoms is according to figure 1. Positive (negative) coordinates denote outward (inward) displacements relative to the average plane of the layer.

	Displacements (Å) for atom number					Overall buckling (Å)
	1	2	3	4	5	
fcc-domain (70%)						
Pb layer	+0.05	+0.01	+0.05	-0.16	-	0.11
Co layer	+0.01	+0.09	+0.03	-0.05	-0.11	0.20
Cu layer	-0.01	-0.07	-0.03	-0.05	+0.07	0.14
hcp-domain (30%)						
Pb layer	+0.06	+0.02	-0.10	-0.04	-	0.16
1st Co layer	-0.14	-0.10	+0.08	+0.08	-0.02	0.22
2nd Co layer	+0.05	-0.01	-0.11	+0.03	-0.07	0.16

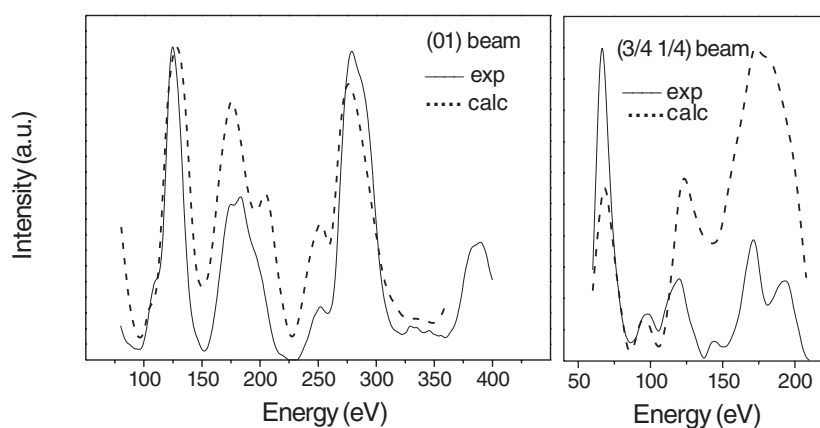


Figure 8. Comparison of experimental and calculated best-fit spectra for a selected integer and fractional order beam of (4×4) -Pb/1.3 ML Co/Cu(111).

make them rather uncertain. The errors typically amount to ± 0.07 Å and ± 0.11 Å in the top layers of the fcc-domain and ‘hcp-domain’ respectively, and increase further with increasing depth. The error margins increase as compared to the 7 ML case in spite of the fact that the quality of the theory–experiment fit is comparable as mirrored by a minimum $R_p = 0.21$ ($\text{var}(R_p) = 0.039$) as well as by a similarly favourable visual comparison displayed in figure 8 for two selected beams. The increase of errors is mainly due to the presence of two domains which makes for the sensitivity of the domain-averaged intensities with respect to an atomic coordinate within a single domain decrease. Yet, though the atomic coordinates exhibit large errors, this does not apply to the same extent to the overall buckling amplitudes of the layers as such buckling is necessary to bring the level of fractional order spot intensities to that experimentally observed. The vertical spacings between the average planes result as $d_{12} = 2.44$ Å, $d_{23} = 2.10$ Å, $d_{34} = 2.08$ Å for the fcc-domain and $d_{12} = 2.40$ Å, $d_{23} = 1.96$ Å, $d_{34} = 1.99$ Å for the ‘hcp-domain’.

5. Discussion

For the discussion of the above results we first address the (4×4) -Pb/7 ML Co/Cu(111) structure and compare it to that of (4×4) -Pb/Cu(111) investigated earlier [9]. In the latter case, i.e. with the substrate strictly fcc-stacked, the Pb overlayer is found to induce a surprisingly strong substrate reconstruction extending down to the third copper layer. The reconstructive relaxation of the layers is a way to reduce the buckling of the lead layer drastically, i.e. from 0.39 Å (for the unreconstructed substrate) to 0.20 Å. Even more, the buckling of the first copper layer is larger than that of the lead layer. Also, there is some inverse corrugation of the lead layer in the sense that the position of the Pb atom residing on top of a copper atom is lower than for all other atoms. The corresponding picture is rather different for the hcp-stacked 7 ML cobalt film: significant buckling applies only to the first cobalt layer and—not surprisingly in view of that—the corrugation of the lead layer (0.34 Å) is only modestly reduced. It exhibits no real inverse corrugation though the depth coordinate of the on-top atom is second to only one other Pb atom, namely that in the fcc-hollow site (see figure 3). The two adsorption phases have in common the fact that the corrugation of the lead and top substrate layers are substantial. For the copper layers of Pb/Cu the large buckling is in agreement with calculations using the embedded atom method (EAM), yet not for the lead layer [7]. However, recent work using density functional theory (DFT) reproduced the large corrugation for all the layers of Pb/Cu [27]. With the two new LEED structure determinations presented in this paper being methodically equivalent to that of our former analysis of Pb/Cu we are confident that the structural features derived are largely correct, too. Of course, final confirmation can only come by the application of independent methods, either experimental or theoretical, or both.

With regard to the scenario for the phase (4×4) -Pb/1.3 ML Co/Cu(111) the overall structural features of both domains are more similar to Pb/Cu than to Pb/7 ML Co/Cu. The buckling of the Pb layer is drastically reduced and the reconstruction extends to at least the second substrate layer. Though buckling of the third substrate layer was not considered, some buckling is likely as the second layer is found to buckle with considerable amplitude. Taking the decay of the buckling from the case of Pb/Cu as a measure one can estimate a third substrate layer-buckling amplitude of the order of 0.06–0.08 Å. For a comparison of the atomic positions we should restrict ourselves to the lead atoms because only their coordinates were retrieved with sufficient accuracy. In fact, an inspection of figures 3, 4 and 7 shows that the lead positions in the fcc-domain of the phase Pb/1.3 ML Co/Cu are rather similar to that in the phase Pb/Cu though the extent of the inverse corrugation is a bit reduced. Consistently, the Pb positions in the ‘hcp-domain’ of the 1.3 ML film exhibit similarities with Pb/7 ML Co/Cu whereby the strong inward displacement of the fcc-hollow site atom is considerably smaller.

With the structural information at hand one can address the question whether the described drastic differences between the cases of Pb/Cu and Pb/7 ML Co/Cu are due more to the different substrate stacking involved or the differences between the chemical species. First we recall that with Co growing on Cu(111) the cobalt film quickly assumes hcp stacking and simultaneously contracts to its native lattice parameter [28]. The latter ($a_{\text{Co}} = 2.50$ Å) is smaller than that of Cu ($a_{\text{Cu}} = 2.55$ Å) so that the lead atoms ($a_{\text{Pb}} = 3.50$ Å) must be compressed more to fit into a (4×4) superstructure on Co than on Cu. This easily explains a smaller buckling of the Pb layer for Pb/Cu compared to Pb/Co and Pb/7 ML Co/Cu. The argument does not hold for the fcc-domain of the 1.3 ML film as this is pseudomorphic with respect to the copper substrate. In contrast, in the ‘hcp-domain’ the stacking fault indicates that the film already starts to be non-pseudomorphic, i.e. to contract according to our earlier investigations

[28]. Additionally, according to the melting temperatures ($T_{\text{Cu}} = 1336 \text{ K}$, $T_{\text{Co}} = 1768 \text{ K}$) the bonding within copper should be weaker than within cobalt. This is consistent with the observation that the buckling in cobalt decays faster towards the bulk than in copper. By all these arguments we tend to make the chemical properties of atoms dominantly responsible for the structures observed. Yet, some influence of the different stacking involved cannot be ruled out. The vertical displacements observed should certainly be affected by the stacking sequence, as in AB. . . stacking atoms in every second layer are on top of each other while this holds only for every third layer for ABC. . . stacking.

So, the scenario for the structural influence of Pb as a surfactant in the growth of Co on Cu(111) seems to be as follows: during the whole growth Pb *always* induces the substrate and/or the growing film to reconstruct. For the copper still uncovered by Co in the initial stage of growth, the reconstruction is most drastic. It affects several layers so that the buckling of the Pb layer can be heavily reduced. With more and more cobalt deposited the character of the reconstructions changes. It increasingly concentrates on the Pb layer and the top film layer only, whereby the Pb layer becomes more strongly buckled. This change of the character of the reconstruction may be attributed to the change from pseudomorphic to non-pseudomorphic growth of Co on Cu(111) with cobalt assuming its native lattice parameter with increasing film thickness. Yet, there might be some influence of the different stacking, too. The reconstruction in the surfactant and top film layer prevails during the full growth which might be connected with the activity of the surface agent Pb. Obviously, the top film layer is induced to behave structurally rather than flexibly by the surfactant as also discussed for Pb/Cu [9]. So, the exchange processes essential for controlling the surface diffusion during growth are favoured, eventually allowing for layer-by-layer growth as observed [10]. Though this conclusion might appear to be a bit speculative, it fits with the experimentally determined structural features of growth.

Acknowledgments

The authors are indebted to the Spanish Ministerio de Educación y Cultura and to Deutscher Akademischer Austauschdienst (DAAD) granting scientific research visits through the program 'Acciones Integradas'. The work in Madrid was supported by the CICyT through project no MAT98-0965-C04-02.

References

- [1] Cabrera N and Vermileya D A 1958 *The Growth of Crystals from Solutions* ed R H Doremus, B W Roberts and D Turnbull (New York: Wiley) p 393
- [2] Camarero J, Ferrón J, Cros V, Gómez L, Vázquez de Parga A L, Gallego J M, Prieto J E, de Miguel J J and Miranda R 1998 *Phys. Rev. Lett.* **81** 850
- [3] Hansen L, Stoltze P, Jacobsen K W and Nørskov J K 1991 *Phys. Rev. B* **44** 6523
- [4] Kellog G L and Feibelman P J 1990 *Phys. Rev. Lett.* **64** 3143
- [5] de Miguel J J, Sánchez A, Cebollada A, Gallego J M, Ferrón J and Ferrer S 1987 *Surf. Sci.* **189190** 1062
- [6] Wulfhekel W, Lipkin N N, Kliewer J, Rosenfeld G, Jorritsma L C, Poelsema B and Comsa G 1996 *Surf. Sci.* **348** 227
- [7] Nagl C, Schmid M and Varga P 1996 *Surf. Sci.* **369** 159
- [8] Braun J and Toennies J P 1996 *Surf. Sci.* **368** 226
- [9] Müller S, Prieto J E, Rath C, Hammer L, Miranda R and Heinz K 2001 *J. Phys.: Condens. Matter* **13** 1793
- [10] Prieto J E, Rath Ch, Müller S, Hammer L, Heinz K and Miranda R 2000 *Phys. Rev. B* **62** 5144
- [11] Camarero J, Spendeler L, Schmidt G, Heinz K, de Miguel J J and Miranda R 1994 *Phys. Rev. Lett.* **73** 2448
- [12] Camarero J, Graf T, de Miguel J J, Miranda R, Kuch W, Zharnikov M, Dittschar A, Schneider C M and Kirschner J 1996 *Phys. Rev. Lett.* **76** 4428

- [13] de la Figuera J, Prieto J E, Ocal C and Miranda R 1993 *Phys. Rev. B* **47** 13043
- [14] Rath Ch, Prieto J E, Müller S, Miranda R and Heinz K 1997 *Phys. Rev. B* **55** 10791
- [15] Prieto J E, de la Figuera J and Miranda R 2000 *Phys. Rev. B* **62** 2126
- [16] Heinz K 1995 *Rep. Prog. Phys.* **58** 637
- [17] Rous P J, Pendry J B, Saldin D K, Heinz K, Müller K and Bickel N 1986 *Phys. Rev. Lett.* **57** 2951
- [18] Rous P J and Pendry J B 1986 *Surf. Sci.* **219** 355, 373
- [19] Rous P J 1992 *Progr. Surf. Sci.* **39** 3
- [20] Blum V and Heinz K 2001 *Comput. Phys. Commun.* **134** 392
- [21] Döll R, Kottcke M and Heinz K 1993 *Phys. Rev. B* **48** 1973
- [22] Heinz K, Döll R and Kottcke M 1996 *Surf. Rev. Lett.* **3** 1651
- [23] Kottcke M and Heinz K 1997 *Surf. Sci.* **376** 352
- [24] Pendry J B 1980 *J. Phys. C: Solid State Phys.* **13** 937
- [25] Ascolani H, Cerda J R, de Andres P L, Miguel J J, Miranda R and Heinz K 1996 *Surf. Sci.* **345** 320
- [26] de la Figuera J, Prieto J E, Kostka G, Müller S, Ocal C, Miranda R and Heinz K 1996 *Surf. Sci.* **349** L139
- [27] Bartelt N *et al* 2000 private communication
- [28] Müller S, Kostka G, Schäfer T, de la Figuera J, Prieto J E, Ocal C, Miranda R, Heinz K and Müller K 1996 *Surf. Sci.* **352–354** 46